

# CorrEmbed: Evaluating Pre-trained Model Image Similarity Efficacy with a Novel Metric

Karl Audun Kagnes Borgersen  
University of Agder  
Grimstad, Norway  
karl.audun.borgersen@uia.no

Morten Goodwin  
University of Agder  
Grimstad, Norway  
morten.goodwin@uia.no

Jivitesh Sharma  
University of Agder  
Grimstad, Norway  
jivitest.sharma@uia.no

Tobias Aasmoe  
Tise  
Oslo, Norway  
tobias@tise.com

Mari Leonhardsen  
Tise  
Oslo, Norway  
mari.leonhardsen@tise.com

Gro Herredsvela Rørvik  
FJONG  
Oslo, Norway  
gro@fjong.com



**Figure 1.** Demonstration of image embedding search. The original image is displayed to the far left, with the most similar images being displayed beside it.

## Abstract

Detecting visually similar images is a particularly useful attribute to look to when calculating product recommendations. Embedding similarity, which utilizes pre-trained computer vision models to extract high-level image features, has demonstrated remarkable efficacy in identifying images with similar compositions. However, there is a lack of methods for evaluating the embeddings generated by these models, as conventional loss and performance metrics do not adequately capture their performance in image similarity search tasks.

In this paper, we evaluate the viability of the image embeddings from numerous pre-trained computer vision models

using a novel approach named CorrEmbed. Our approach computes the correlation between distances in image embeddings and distances in human-generated tag vectors. We extensively evaluate numerous pre-trained Torchvision models using this metric, revealing an intuitive relationship of linear scaling between ImageNet1k accuracy scores and tag-correlation scores. Importantly, our method also identifies deviations from this pattern, providing insights into how different models capture high-level image features.

By offering a robust performance evaluation of these pre-trained models, CorrEmbed serves as a valuable tool for researchers and practitioners seeking to develop effective, data-driven approaches to similar item recommendations in fashion retail.<sup>1</sup>

**CCS Concepts:** • Computing methodologies → Image representations; Neural networks.

**Keywords:** Image Similarity, Content-Based Recommendations, Zero-Shot Learning, Recommender Systems

## ACM Reference Format:

Karl Audun Kagnes Borgersen, Morten Goodwin, Jivitesh Sharma, Tobias Aasmoe, Mari Leonhardsen, and Gro Herredsvela Rørvik.

<sup>1</sup>All code and experiments are openly available at <https://anonymous.4open.science/r/CorrEmbedRecSys-731F>

Permission to make digital or hard copies of all or part of this work for personal or classroom use is granted without fee provided that copies are not made or distributed for profit or commercial advantage and that copies bear this notice and the full citation on the first page. Copyrights for components of this work owned by others than ACM must be honored. Abstracting with credit is permitted. To copy otherwise, to republish, to post on servers or to redistribute to lists, requires prior specific permission and/or a fee. Request permissions from [permissions@acm.org](mailto:permissions@acm.org).

AI-2023, Dec 12–14, 2023, Cambridge, England

© 2023 Association for Computing Machinery.

ACM ISBN 978-x-xxxx-xxxx-x/YY/MM. . \$15.00

<https://doi.org/XXXXXXX.XXXXXXX>

2023. CorrEmbed: Evaluating Pre-trained Model Image Similarity Efficacy with a Novel Metric. In *Proceedings of AI-2023 Forty-third SGAI International Conference on Artificial Intelligence (AI-2023)*. ACM, New York, NY, USA, 9 pages. <https://doi.org/XXXXXXX.XXXXXX>

## 1 Introduction

There are several enticing aspects to using pre-trained computer vision models to recommend similar products. It requires no resources for model training, avoiding the need for labeled data or the computation required to train machine learning models. Neither does it require any product information beyond a product image, lending itself particularly well to relatively small online storefronts or online second-hand sales. Similar item recommendations entail simply recommending items similar to a target item. Fashion, in particular, as a domain has some distinctive properties that make it uniquely suited for recommendations based on image similarity search, namely its emphasis on the visual appearance of the products. Extracting image embeddings from pre-trained models for Recommender Systems(RS) is used in production today. Tise<sup>2</sup>, for instance, is a large Norwegian second-hand sales company and the employer of two of our co-authors. The company used embedding comparisons in production as part of an ensemble similar-item recommendation method.

However, existing methods face validation challenges because direct comparisons of image embeddings do not align with the intended use case of pre-trained image models. Consequently, neither their loss nor classification performance metrics effectively indicate a model's performance in this domain. While the efficacy of retrieving similar images based on computer vision model embeddings is apparent to human observers, limited literature exists on evaluating their effectiveness. This paper contributes a more rigorous evaluation of how well each of the models performs as compared to human tag annotation.

This paper introduces CorrEmbed, an evaluation metric based on tag-based similarity within the fashion domain. It takes advantage of human-tagged outfits to evaluate the zero-shot performance of a model's embeddings. The evaluation is performed by calculating the correlation between distances in image-embedding space and in tag-embedding space. These indicator variables, or tag vectors, are augmented by weighting them according to category using statistical entropy.

CorrEmbed is used to provide a benchmark for the performance of numerous pre-trained computer-vision models. We discuss the performance of these and which features and model architectures are more conducive to good tag-correlation performance, such as the format of the tensors

produced by different pre-trained model versions. In particular, we underline cases in which this performance deviates from the pattern of increased image-classification performance leading to increased CorrEmbed performance.

The pre-trained models evaluated for this project are from Torchvision's model set[16].

## 2 Related Work

RS can refer to numerous different approaches, from Collaborative Filtering[13] to Deep Learning[20][5] to (Deep) Reinforcement Learning[1] to Tsetlin Machines[3]. At the core of this paper lies the concept of similar item recommendations. While collaborative filtering models have long been the dominant method for providing recommendations, content-based RSs have often been employed to address problems with linear scaling. These item-based RSs identify relationships between items and recommend items frequently bought together, for which the capability of extracting information from for example text descriptions or images is highly relevant[12]. Image embeddings have also been used in the context of classification for a while. Akata et al.[2] use it to perform zero-shot learning on unsupervised data by detecting clusters of image embeddings. Fu. et al. [6] provide an overview of zero-shot learning in 2019. These papers demonstrate how prevalent the use of image embeddings is in the SotA.

Visual image attributes form the foundation of numerous contemporary RSs, such as [8] and [25]. Evaluating how similar images are is a necessity within Image Retrieval, in this context, Tarasov et al.[22] utilize the embeddings of a trained neural network for this task for which the distance between two images is the Euclidian distances between embeddings. Garcia et al.[7] train a regression NN for this purpose and compare performance to a few other metrics, including cosine distance. Resnick et al. [18] utilize Pearson correlation to measure user similarity. While these previous works parse image (or user) embeddings in a manner comparable to CorrEmbed, none of them quantitatively evaluate how well individual models perform at measuring image similarity.

## 3 Methods

In summary, CorrEmbed entails retrieving image embeddings from pre-trained classification computer vision models and identifying similar items by calculating the distance between them. We evaluate their performance by calculating the correlation of the distances between pairs of image embeddings and the distances between pairs of tag embeddings. The final score represents the mean correlation between image and tag embeddings across  $k$  samples.

The datasets used in this paper are generated using data from FJONG, a small clothing rental company with access to approximately 10,000 human-tagged outfits and around

<sup>2</sup>Tise: [tise.com](https://tise.com)

18,000 corresponding images. 705 tags constitute the tag-embedding space, each belonging to one out of the 13 tag categories listed in Table 1.

All models and model weights are retrieved from Torchvision’s model set<sup>3</sup>. All classification models have trained on the ImageNet[19] dataset with 1k classes.

### 3.1 Tag-Based metric

A one-hot-encoded vector of tags is calculated based on tag presence, resulting in a vector with 705 dimensions. Similarly to the image-embeddings, the clothing items are converted into tag-based representations. We calculate the distances between an input embedding  $i$  and all  $n$  other embeddings for both tag and image embeddings. (Eq. 1,3,2) in which  $T$  and  $I$  refer to a set of all image and tag embeddings respectively and  $T_i$  or  $I_i$  represents the  $i$ th element in both of these sets. For a given set of image embeddings, we assess the performance by calculating the correlation between the tag-based metric distance and the distance between image embeddings. This is done using the Pearson correlation coefficient. The final score for a model is obtained by computing the mean correlation across  $k$  image samples (Eq. 4). In which  $x_i$  and  $y_i$  represent a set of  $n$  tag and image similarity scores for the vector at index  $i$  and  $\bar{x}$  and  $\bar{y}$  are the mean values of the same sets.

$$\text{cosine\_similarity}(\mathbf{A}, \mathbf{B}) = \frac{\mathbf{A} \cdot \mathbf{B}}{\|\mathbf{A}\| \|\mathbf{B}\|} \quad (1)$$

$$\text{Image\_Similarity}(I_i) = y_i = \{\text{cosine\_similarity}(\mathbf{I}_i, \mathbf{I}_j) : j = 1, 2, \dots, n\} \quad (2)$$

$$\text{Tag\_Similarity}(T_i) = x_i = \{\text{cosine similarity}(\mathbf{T}_i, \mathbf{T}_j) : j = 1, 2, \dots, n\} \quad (3)$$

$$\text{CorrEmbed} = \frac{1}{k} \sum_{i=1}^k \frac{\sum_{j=1}^n (x_{ji} - \bar{x})(y_{ji} - \bar{y})}{\sqrt{\sum_{j=1}^n (x_{ji} - \bar{x})^2} \sqrt{\sum_{j=1}^n (y_{ji} - \bar{y})^2}} \quad (4)$$

In this dataset, tags are grouped into categories, e.g., “Collar” is categorized as “Neckline”. All tags present in the dataset, except for brand tags, are shown in Table 1. As the “Size” and “Shoe Size” category isn’t necessarily present in the images of the dataset (The same clothing item in different sizes will occasionally share the same product photo), this category is dropped entirely. For the context of recommendation, some tags are more compelling to the average customer than others. We are more interested in representations that appropriately capture the user’s interests. A user browsing for a new winter coat will be more interested in other winter coats rather than products with the same color. We evaluate the customers’ purchase history and compute the entropy

for each tag category. Calculating the entropy was done to capture the likelihood of a customer re-purchasing an item with a similar category, yielding a lower value if the purchased outfits’ tag categories exhibit consistent sub-tags. For example, if a user exclusively buys clothing items with “Dots” or “Stripes” patterns, the “Pattern” category will have a low entropy score. Conversely if the user prefers a variety of colors, the “Color” category will have a high entropy score. As shown in Equation 5, in which  $C_i$  refers to a customer’s rental history,  $c$  is the total number of customers evaluated,  $C_i(x_j)$  is the total occurrences of tag  $x_j$  in the rental history  $C_i$ , and  $X$  refers to a tag category for which we want to calculate the weights.

$$\text{Entropy}(X) = H(X) = \frac{1}{c} \sum_{i=1}^c - \sum_{j=1}^{|X|} \frac{C_i(x_j)}{\|C_i\|} \log \frac{C_i(x_j)}{\|C_i\|} \quad (5)$$

We normalize these entropy values between 0 and 1 based on the maximum possible entropy within this range, and subsequently invert the weights (Eq. 6),  $\min(H)$  and  $\max(H)$  refer to the largest and smallest calculated tag category value. Our earlier tag embeddings are then weighted for their respective tag category. This ensures, for example, that the relative tag distance between a blue blazer and a red blazer is shorter than the distance between a blue blazer and a blue jumpsuit.

$$\text{Tag\_Weights}(X) = 1 - \frac{H(X) - \min(H)}{\max(H) - \min(H)} \quad (6)$$

## 4 Results and Discussions

This section presents the results of our experiments, which benchmark the performance of our pre-trained models. We also employ t-Distributed Stochastic Embedding (t-SNE) plots to visualize the clustering of embeddings in our models.

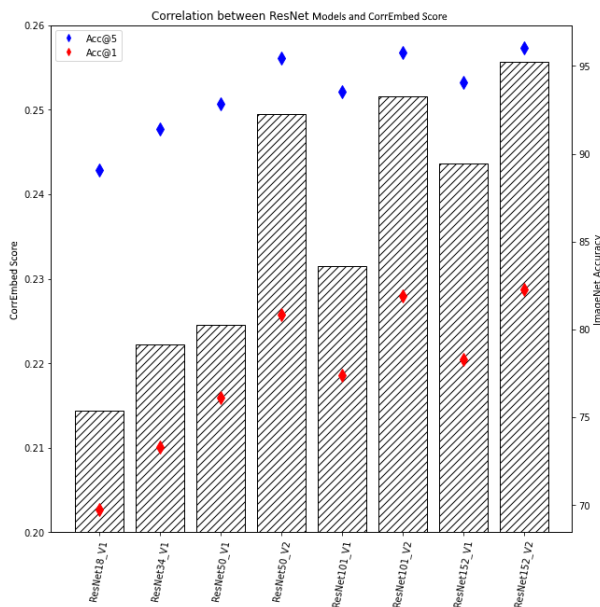
Model performance on CorrEmbed generally increases by the model size and ImageNet performance, as seen in Figure 2. While model performance doesn’t necessarily directly scale in accordance with its ImageNet score, scaled-up versions of the same model outperform their smaller counterparts. This provides a good sanity check on the veracity of our metric. The correlation between the ImageNet score and the CorrEmbed score holds true for comparisons between the scaled-up versions of the same architecture but isn’t necessarily the case when comparing two different model architectures. For instance, EfficientNet models outperform ResNet models with the same accuracy score, e.g., ResNet50 V2 has an Acc@1 score of 80.858 and achieves a CorrEmbed score of 0.249, as compared to EfficientNet B2 which has an Acc@1 score of 80.608 and a CorrEmbed score of 0.273.

Table 2 (and Figure 3) provides an overview of the performance of various model architectures. We selected the

<sup>3</sup>TorchVision’s model set is available at <https://pytorch.org/vision/stable/models.html>

Category	Tags
Brand	552 different fashion brands, omitted for brevity.
Material	Triacetate, Lyocell, Polyester, Cashmere, Linen, Cupro, Velvet, Leather, Spandex, Lace, Beaded, Faux fur, Fur, Rayon, Down, Acrylic, Bamboo, Polyethylene Terephthalate, Acetate, Satin, Chiffon, Silk, Polyamide, Tulle, Wool, Nylon, Denim, Cotton, Vegan Leather, Viscose, Modal, Gold, Elastane, Lurex, Lycra, Lacquer, Silver, Tencel, Polyvinyl Chloride, Polyurethane, Metal
Category	Blouses, Accessories, Jewelry, Shirts, Kimonos, Shoes, Bags, Pants, Suits, Coats, Sweaters, Vests, Outerwear, Jumpsuits, Skirts, Blazers, Dresses, Cardigans, Knitwear, Jackets, Shorts, Tops
Color	Yellow, Purple, Grey, Blue, Green, Brown, Pink, Multicolor, Beige, Orange, Black, Gold, Red, White, Navy, Silver, Turquoise, Burgundy
Size	XXS, Onesize, Large, 4XL, Medium, Extra Small, 3XL-4XL, Extra Large, 3XL, Small, 2XL, XXL-XXXXL
No category	Sporty, Winter, Height - 180-190 cm, Dressed-up, Fall, New, Summer, Romantic, Edgy, Spring, Classic
Occasion	FJONG Active, Going out, Black-tie, Everyday, FJONG Plus Size, Prom, Wedding, Party, FJONG Bump, Active, Business
Sleeve	Mid arms, Spaghetti straps, T-shirt, Cold shoulder, Tube, Straps, Long arms
Embellishment	Ruffles, Pearls, Sequins, Feathers, Glitter, Studs, Tassels
Neckline	Boat Neck, Deep Neck, Halter Neck, V-neck, Round Neck, Collar, Turtleneck
Waist	Empire, High, Normal, Adjustable, Stretchy, Low
Shoe Size	39, 36, 40, 38, 37, 41
Pattern	Floral, Checkers, Dots, Stripes, Animal, Pattern
Fit	Loose fit, Wrap, Pregnant-friendly, Slim fit
Length	Midi, One, Mini, Maxi

**Table 1.** Tags present in the dataset of this paper



**Figure 2.** Comparison between ResNet [9] model correlation score and ImageNet1k accuracy across differing ResNet model sizes. CorrEmbed scores have been constrained to the range of 0.2 to 0.26 to emphasize the score differences.

top-performing version of each architecture based on ImageNet1k accuracy. We include two control methods for both tag and image embeddings to establish a baseline for significance. The first random model method generates a random tensor with the same shape as the image embeddings for each image, while the random tag vectors generate a binary vector with the same shape as the tag vector. The two shuffle control methods randomize the association between tag or image embeddings and each outfit.

We observe a significant correlation between ImageNet1k scores and CorrEmbed scores, albeit with some deviations.

The top-performing models ViT, RegNetY[17], and EfficientNet[21] outperform other models by a margin comparable to the performance improvements between AlexNet[14] and ConvNext[15], despite negligible differences in ImageNet1k scores. This observation makes some intuitive sense, as improving a model’s accuracy score from, for instance, 87 to 88 likely corresponds to a much greater enhancement of the model’s internal representation than an improvement from 56 to 57, in line with the Pareto Principle<sup>4</sup>. However, the observed increase in performance exceeds what we would expect if this were the sole contributing factor.

The embeddings evaluated in this case were all retrieved as the standard output embeddings of the models. This had the added advantage of removing the shape of the embeddings as a factor for the CorrEmbed score since the final output embedding of the classes remains the same 1000-dimensional vector regardless of the model architecture.

The layers preceding the output layer tend to capture a finer representation of the embeddings. Though the degree to which this is the case depends on the model itself. Table 3 details the scores of the models based on the input embeddings to the penultimate layer rather than the output. Working with embeddings earlier than this is unfortunately too inconsistent to make any direct comparisons. As happened with SqueezeNet[11] in Table 3, any embeddings retrieved before the model pools into the shape (1, -1) tend to reach unworkable sizes.

Table 3 also logs inference time for batches of 90 images, along with the shapes of the evaluated tensors. Unsurprisingly, the best-performing models also clocked in the longest inference time, though in contrast to ImageNet accuracy, some models surpassed expectations significantly based solely on inference time. MaxViT[23] and MobileNet[10] are good examples of these. An explanation for this could be the priorities of the original model developers. As we’ve only

<sup>4</sup>[https://en.wikipedia.org/wiki/Pareto\\_principle](https://en.wikipedia.org/wiki/Pareto_principle)

Model	ImgNet Acc@1	ImgNet Acc@5	CorrEmbed	Unweighted	Random	Shuffled
random	0.0	0.0	0.0086	0.0088	0.0229	0.008
random shuffle	0.0	0.0	0.0016	-0.0032	0.0076	-0.0058
AlexNet	56.522	79.066	0.1463	0.1485	0.0165	0.0008
SqueezeNet1 1	58.178	80.624	0.1508	0.137	0.012	0.0038
GoogLeNet	69.778	89.53	0.2103	0.1933	0.0133	0.0036
VGG19 BN	74.218	91.842	0.1837	0.1733	0.0129	0.0023
MobileNet V3 Large	75.274	92.566	0.2251	0.201	0.0174	0.0048
ShuffleNet V2 X2	76.23	93.006	0.2264	0.1977	0.0175	0.0051
DenseNet201	76.896	93.37	0.2121	0.1903	0.0146	0.0023
MNASNet1 3	76.506	93.522	0.2276	0.2083	0.0148	0.0058
Wide ResNet101 2	81.602	95.758	0.2445	0.2182	0.0075	0.0034
resnet152 V2	82.284	96.002	0.2493	0.2243	0.0119	0.0043
ResNeXt101 64X4D	83.246	96.454	0.2393	0.2092	0.0096	0.0048
MaxViT T	83.7	96.722	0.1943	0.174	0.0044	0.0039
Swin V2 B	84.112	96.864	0.2649	0.2417	0.0151	0.0045
ConvNext Large v1	84.414	96.976	0.2641	0.2383	0.0157	0.0032
EfficientNet V2 L	85.808	97.788	<b>0.3680</b>	<b>0.3189</b>	0.0176	0.0051
RegNet Y 32GF	86.838	98.362	0.3428	0.306	0.014	0.0038
ViT H 14 E2E	<b>88.552</b>	<b>98.694</b>	0.3633	0.3184	0.0114	0.0036

**Table 2.** Overview of the performance using the top-performing version of each model architecture, sorted by ImageNet1k score. ImgNet Acc@1 and ImgNet Acc@5 refer to the model’s performance on accuracy at ImageNet1k top 1 and top 5, respectively. CorrEmbed is our weighted tag vector scoring, and unweighted refers to the same vectors without the weights. Random and shuffle in both rows and columns are control methods. The CorrEmbed scores of this table are visually represented in Figure 3

evaluated the top-performing models of each architecture, these are likely the model iterations with the heaviest focus on performance to the detriment of other aspects of the model and are, therefore, subject to a significant degree of diminishing returns. Interestingly, despite the varying tensor shapes, the CorrEmbed score is even more closely associated with the ImageNet1k score in the penultimate model layers (Table 2 compared to the output layer in Table 3, have a Pearson correlation of 0.767 and 0.941 respectively compared to ImageNet *accuracy@1*)

The use of models trained on ImageNet, in particular, could potentially have had the added advantage of the models ignoring any humans appearing in the image. For example, the 4<sup>th</sup> most similar image detected by the upper model in Figure 5. As none of ImageNet1k’s classes involve classifying humans[19], the pre-trained models are incentivized to ignore them. This congrues well with our metrics emphasizing the properties of worn clothing rather than the people wearing them. The ability to overlook the human subjects in images is more pronounced in the stronger models compared to the weaker ones.

#### 4.1 Evaluating Fashion-CLIP

To gain a better idea of how well the ImageNet1k models perform as compared to other models, we run CorrEmbed on Fashion-CLIP[4], an open vocabulary model fine-tuned on the fashion domain. The model achieved a score of 0.396 as compared to our top-performing model of ViT\_H\_14\_E2E,

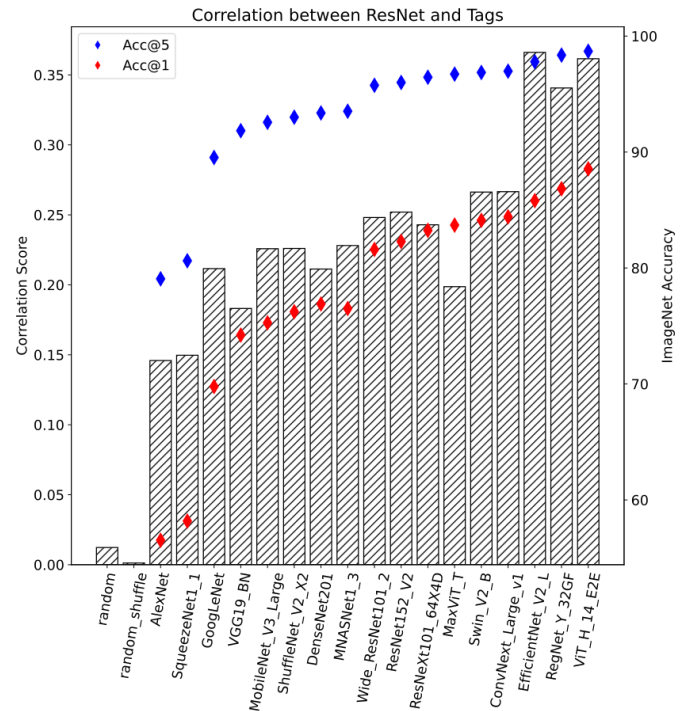


**Figure 3.** Graph representation of the results from Table 2. Columns display the CorrEmbed score for the different models. The blue and red lines show performance on ImageNet

Model	Model Params	CorrEmbed	Inference Time	Embedding Shape
AlexNet	61.1M	0.1775	0.052	(90, 4096)
SqueezeNet1 1	1.2M	N/A	0.094	(90, 1000, 13, 13)
GoogLeNet	6.6M	0.2167	0.064	(90, 1024)
VGG19 BN	143.7M	0.2247	0.158	(90, 4096)
MobileNet V3 Large	5.5M	0.2299	0.054	(90, 1280)
ShuffleNet V2 X2	7.4M	0.2290	0.057	(90, 2048)
DenseNet201	20.0M	0.2406	0.151	(90, 1920)
MNASNet1 3	6.3M	0.2375	0.079	(90, 1280)
Wide ResNet101 2	68.9M	0.2462	0.264	(90, 2048)
resnet152 V2	60.2M	0.2491	0.202	(90, 2048)
ResNeXt101 64X4D	83.5M	0.2469	0.608	(90, 2048)
MaxViT T	30.9M	0.2516	0.197	(90, 512)
Swin V2 B	87.9M	0.2659	0.404	(90, 1024)
ConvNext Large v1	197.8M	0.2695	0.559	(90, 1536)
EfficientNet V2 L	118.5M	0.3604	1.022	(90, 1280)
RegNet Y 32GF	145.0M	0.3824	1.137	(90, 3712)
ViT H 14 E2E	633.5M	<b>0.4288</b>	15.412	(90, 1280)

**Table 3.** Overview of CorrEmbed performance based on the input to the last layer. Inference time is the time taken to evaluate  $\frac{1}{200}$ th of the dataset (90 images). Control values for both image and tag embeddings, along with binary tag vectors have been omitted for brevity. These maintain roughly the same ratio to the CorrEmbed score as seen in Table 2. As the final layer of SqueezeNet is an Average Pooling layer, we were unable to perform our experiment on it due to the size of the tensors it produced. The inference time documented for ViT was run in a separate batch from the rest of the models shown. It is, therefore, possible external factors have influenced it.

which achieved a score of 0.471<sup>5</sup>. Interestingly, the Fashion-CLIP model performs worse than ViT\_H despite being fine-tuned to the relevant domain.

## 4.2 Exploring embedding space

As shown in Figure 4, the high-dimensional embeddings of each image can be visualized in low-dimensional space by taking into account the relative distances between each point using t-SNE[24]. Despite the models used not being trained in this domain we observe some clear clustering of embeddings based on their tags. Figure 4 label embeddings tagged with the same “category” (essentially, the type of clothing). Moreover, we notice significant improvements in clustering for the better-performing model on the right compared to the model on the left.

An expected flaw with recommending similar items using embeddings is evident in the t-SNE diagrams. Some embeddings are naturally going to end up in isolated positions far away from the larger clusters of embeddings. These isolated items will effectively never be recommended based solely on similar item recommendations. Steps can be taken to increase the recommendation priority of these isolated items, but embeddings placed on the outskirts of clusters will likely rank

far too low in the similar item rankings among its neighbors to ever actually be recommended in a natural setting.

## 4.3 Dataset Scale

The dataset used for this paper is relatively small, consisting of around 18000 images in total. This scale ensures that the direct comparison of all image embeddings is feasible even in production when used for similar item recommendations. However, this format also leads to a significant number of outlier compositions. A good example is the input image in Figure 7. The top-performing model picks up on the worn fleece sweater and finds other warm clothing items to be the most similar, while the lower-performing models are more affected by composition. This makes some intuitive sense. Each image in the ImageNet1k dataset consists of a central subject to be classified and more-or-less irrelevant background information. The better-performing models are the ones able to adequately capture these subjects while avoiding getting hung up on the other details of the images. It is difficult to tell the degree to which the models are affected by the composition, as the majority of the FJONG dataset consists of images with uniform backgrounds and often without a fashion model. A more expansive dataset would better demonstrate how badly composition impacts similarity predictions.

Further, the tagging of outfits within FJONG is significantly noisier than we would prefer. The process of tagging

<sup>5</sup>This experiment was performed on a later iteration of the dataset with significantly reduced noise, this results in somewhat inflated CorrEmbed scores as compared to the scores in Table 2

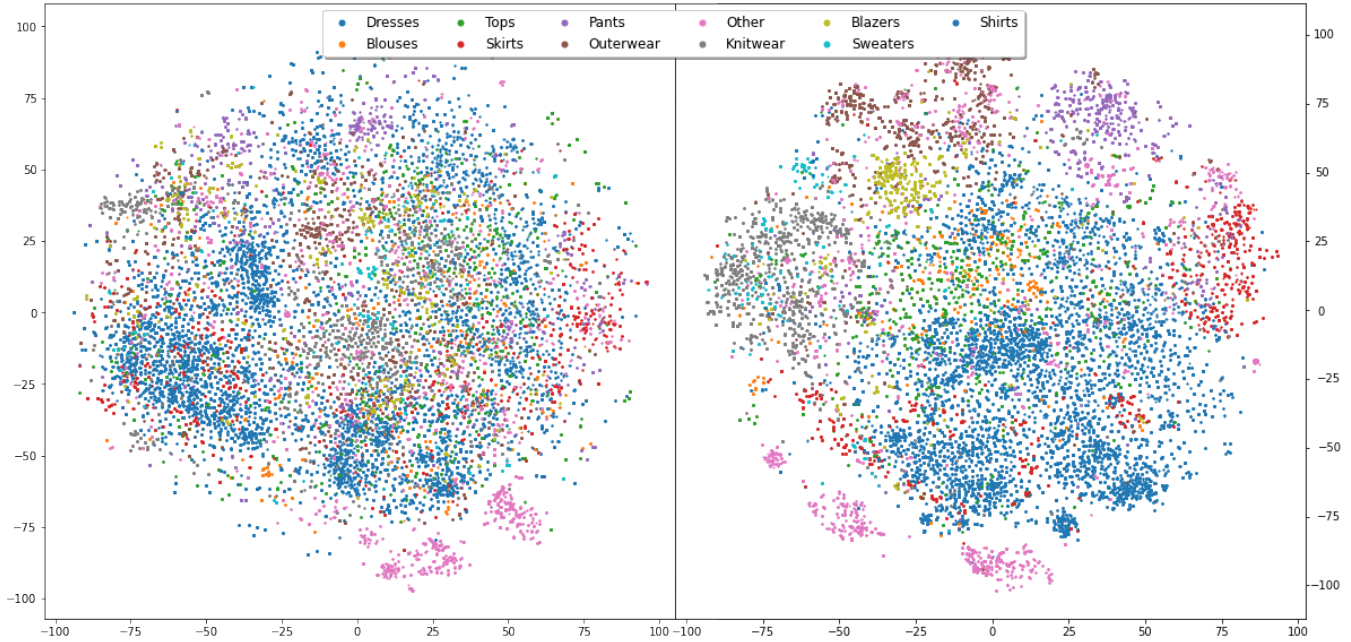


**Figure 4.** t-SNE diagrams of our dataset’s images based on embeddings generated using ResNet50 V1 (left) and ViT H E2E (right). The embeddings are colored according to the “Category” tag category. Only the top 10 categories are shown to maintain legibility. All others are relegated to the “Other” category.

them has been carried out over several years by several different individuals. Therefore, whether and how certain categories of tags, such as “Color” or “Material” has been applied is somewhat inconsistent. While we have not applied CorrEmbed to any other fashion datasets, the noise present in our current one is a good indication of transferability to more thoroughly vetted datasets.

#### 4.4 Qualitative performance analysis

The main purpose of this paper is to achieve a concrete metric with which the capabilities of embedding evaluation could be measured. Such a metric is of little use, however, if the image similarity does not improve in the eyes of a human as well. This section discusses a few qualitative observations concerning the capabilities of higher-performing methods as compared to lower-performing ones. Figure 6 emphasizes how strong the contrast between the best and worst performing models, ViT\_H\_14\_E2E and AlexNet, can be. The former model can easily pick out a set of similar sweaters, while the latter gets bogged down picking out clothes with similar color schemes. Significant differences exist in the attributes that the models choose to focus on, as illustrated in Figure 5. Weaker models tend to put too much emphasis on whether a fashion model is present in the image, as well as the model’s pose. Stronger models, on the other hand, are more capable of ignoring these factors and, for instance, picking out the original clothing item worn in the input image.

The input image in Figure 7 is among the most challenging images in the dataset. The uncommon composition introduces a degree of visual noise, which causes difficulties with image embedding comparison. The extent to which the visual noise affects the embeddings varies. For example, the products identified by the *vgg16* model appear close to random, while the outfits found by the *ViT<sub>H</sub>* model focus on the fleece sweater. Note that the actual product sold from the input image is, in reality, the skirt, not the sweater. This highlights another limitation of this method, the inability to specify which component of the image is most relevant.

## 5 Conclusion

In this paper, we introduce and evaluate the performance of CorrEmbed, a novel method designed to assess the zero-shot image-embedding similarity performance of NNs. We employ this metric to evaluate a myriad of different pre-trained ImageNet1k classification models. Of these models, the vision transformer ViT\_H\_14\_E2E is found to be the most performant, beyond even the performance of Fashion-CLIP, a model tuned to the fashion domain. CorrEmbed score is strongly correlated to ImageNet1k performance. While CorrEmbed performance naturally tends to increase for each successive layer of a model, the final output layer is found to produce consistently worse embeddings than the second to last layer. We note that specific model architectures tend to surpass others with comparable performance on ImageNet.



**Figure 5.** Comparison between a strong and weak model. The original image is displayed to the far left, with the most similar images being displayed in order from left to right. The top row shows the stronger ViT\_H\_14\_E2E model while the row below shows the results from the weaker AlexNet model.



**Figure 6.** Comparison between a strong and weak model. The original image is displayed to the far left, with the most similar images being displayed in order from left to right. The top row shows the stronger ViT\_H\_14\_E2E model while the row below shows the results from the weaker AlexNet model.



**Figure 7.** Comparison between ViT\_H (top), resnet50\_v2 (middle), and vgg16 (bottom) with a difficult image. The ViT performs better than the resnet50 model which perform better than the vgg16 model.

For example, Torchvision’s v2 models consistently outperform their v1 counterparts. This study contributes valuable insights into the performance of various models in the context of image-embedding similarity. Though perhaps few surprising conclusions can be drawn from the results, formal evaluation compared to human annotators is an important step to ensure our RSs are as rigorous as possible.

## 6 Acknowledgments

Funded by the Research Council of Norway through the project “Your green, smart and endless wardrobe”, project

number 309977. We thank FJONG for providing the data used as a basis for the dataset in this paper.

## References

- [1] M Mehdi Afsar, Trafford Crump, and Behrouz Far. 2022. Reinforcement learning based recommender systems: A survey. *Comput. Surveys* 55, 7 (2022), 1–38.
- [2] Zeynep Akata, Scott Reed, Daniel Walter, Honglak Lee, and Bernt Schiele. 2015. Evaluation of Output Embeddings for Fine-Grained Image Classification. In *Proceedings of the IEEE Conference on Computer Vision and Pattern Recognition (CVPR)*. IEEE, San Juan, PR, USA, 10 pages.
- [3] Karl Audun Borgersen, Morten Goodwin, and Jivitesh Sharma. 2023. A Comparison Between Tsetlin Machines and Deep Neural Networks

- in the Context of Recommendation Systems. *Northern Lights Deep Learning Workshop* 4 (2023), 8 pages. <https://doi.org/10.7557/18.6807>
- [4] Patrick John Chia, Giuseppe Attanasio, Federico Bianchi, Silvia Terragni, Ana Rita Magalhães, Diogo Goncalves, Ciro Greco, and Jacopo Tagliabue. 2022. Contrastive language and vision learning of general fashion concepts. *Scientific Reports* 12, 1 (2022), 18958. <https://doi.org/10.1038/s41598-022-26364-y>
  - [5] Aminu Da’u and Naomie Salim. 2020. Recommendation system based on deep learning methods: a systematic review and new directions. *Artificial Intelligence Review* 53, 4 (2020), 2709–2748.
  - [6] Yanwei Fu, Tao Xiang, Yu-Gang Jiang, Xiangyang Xue, Leonid Sigal, and Shaogang Gong. 2018. Recent Advances in Zero-Shot Recognition: Toward Data-Efficient Understanding of Visual Content. *IEEE Signal Processing Magazine* 35, 1 (2018), 112–125. <https://doi.org/10.1109/MSP.2017.2763441>
  - [7] Noa Garcia and George Vogiatzis. 2019. Learning non-metric visual similarity for image retrieval. *Image and Vision Computing* 82 (2019), 18–25.
  - [8] Raul Gomez Bruballa, Lauren Burnham-King, and Alessandra Sala. 2022. Learning Users’ Preferred Visual Styles in an Image Marketplace. In *Proceedings of the 16th ACM Conference on Recommender Systems*. ACM, New York, NY, USA, 466–468.
  - [9] Kaiming He, Xiangyu Zhang, Shaoqing Ren, and Jian Sun. 2016. Deep residual learning for image recognition. In *Proceedings of the IEEE conference on computer vision and pattern recognition*. IEEE, New York, NY, USA, 770–778.
  - [10] Andrew Howard, Mark Sandler, Grace Chu, Liang-Chieh Chen, Bo Chen, Mingxing Tan, Weijun Wang, Yukun Zhu, Ruoming Pang, Vijay Vasudevan, et al. 2019. Searching for mobilenetv3. In *Proceedings of the IEEE/CVF international conference on computer vision*. IEEE, New York, NY, USA, 1314–1324.
  - [11] Forrest N Iandola, Song Han, Matthew W Moskewicz, Khalid Ashraf, William J Dally, and Kurt Keutzer. 2016. SqueezeNet: AlexNet-level accuracy with 50x fewer parameters and < 0.5 MB model size. *arXiv preprint arXiv:1602.07360* 1, 1 (2016), 13 pages.
  - [12] George Karypis. 2001. Evaluation of item-based top-n recommendation algorithms. In *Proceedings of the tenth international conference on Information and knowledge management*. ACM, New York, NY, USA, 247–254.
  - [13] Yehuda Koren, Steffen Rendle, and Robert Bell. 2021. Advances in collaborative filtering. *Recommender systems handbook* 1, 1 (2021), 91–142.
  - [14] Alex Krizhevsky, Ilya Sutskever, and Geoffrey E Hinton. 2017. Imagenet classification with deep convolutional neural networks. *Commun. ACM* 60, 6 (2017), 84–90.
  - [15] Zhuang Liu, Hanzi Mao, Chao-Yuan Wu, Christoph Feichtenhofer, Trevor Darrell, and Saining Xie. 2022. A convnet for the 2020s. In *Proceedings of the IEEE/CVF Conference on Computer Vision and Pattern Recognition*. IEEE, New York, NY, USA, 11976–11986.
  - [16] TorchVision maintainers and contributors. 2021. Models and Pre-Trained Weights. <https://pytorch.org/vision/stable/models.html#models-and-pre-trained-weights>. Accessed: 2023-01-17.
  - [17] Ilija Radosavovic, Raj Prateek Kosaraju, Ross Girshick, Kaiming He, and Piotr Dollár. 2020. Designing network design spaces. In *Proceedings of the IEEE/CVF conference on computer vision and pattern recognition*. IEEE, Seattle, WA, USA, 10428–10436.
  - [18] Paul Resnick, Neophytos Iacovou, Mitesh Suchak, Peter Bergstrom, and John Riedl. 1994. Grouplens: An open architecture for collaborative filtering of netnews. In *Proceedings of the 1994 ACM conference on Computer supported cooperative work*. ACM, New York, NY, USA, 175–186.
  - [19] Olga Russakovsky, Jia Deng, Hao Su, Jonathan Krause, Sanjeev Satheesh, Sean Ma, Zhiheng Huang, Andrej Karpathy, Aditya Khosla, Michael Bernstein, et al. 2015. Imagenet large scale visual recognition challenge. *International journal of computer vision* 115 (2015), 211–252.
  - [20] Iqbal H Sarker. 2021. Deep learning: a comprehensive overview on techniques, taxonomy, applications and research directions. *SN Computer Science* 2, 6 (2021), 1–20.
  - [21] Mingxing Tan and Quoc Le. 2021. Efficientnetv2: Smaller models and faster training. In *International conference on machine learning*. PMLR, Cambridge MA: JMLR, Cambridge Massachusetts, USA, 10096–10106.
  - [22] Andrey S Tarasov, Valentina Yu Tarasova, Natalya N Grinchenko, and Maxim A Stepanov. 2020. Development of a Search System for Similar Images. In *2020 ELEKTRO*. IEEE, 1–6.
  - [23] Zhengzhong Tu, Hossein Talebi, Han Zhang, Feng Yang, Peyman Milanfar, Alan Bovik, and Yinxiao Li. 2022. Maxvit: Multi-axis vision transformer. In *Computer Vision—ECCV 2022: 17th European Conference, Tel Aviv, Israel, October 23–27, 2022, Proceedings, Part XXIV*. Springer, Springer Cham, Tel Aviv, Israel, 459–479.
  - [24] Laurens Van der Maaten and Geoffrey Hinton. 2008. Visualizing data using t-SNE. *Journal of machine learning research* 9, 11 (2008), 27 pages.
  - [25] Shuai Zhang, Lina Yao, Aixin Sun, and Yi Tay. 2019. Deep Learning Based Recommender System: A Survey and New Perspectives. *ACM Comput. Surv.* 52, 1, Article 5 (feb 2019), 38 pages. <https://doi.org/10.1145/3285029>